HHS Public Access

Author manuscript

Cancer Genet. Author manuscript; available in PMC 2021 January 01.

Published in final edited form as:

Cancer Genet. 2020 January ; 240: 5–14. doi:10.1016/j.cancergen.2019.10.005.

High-resolution copy number analysis of clear cell endometrial carcinoma

Andrea J. O'Hara[a], **Matthieu Le Gallo**[a], **Meghan L. Rudd**[a], **Daphne W. Bell**[a]

[a]Cancer Genetics and Comparative Genomics Branch, National Human Genome Research Institute, National Institutes of Health, Bethesda, MD 20892, USA

Abstract

Uterine cancer is the 6th leading cause of cancer death amongst American women. Most uterine cancers are endometrial carcinomas (ECs), which are classified into histological subtypes including endometrioid, serous, and clear cell ECs. Somatic copy number alterations (SCNAs) are frequent in serous EC, infrequent in endometrioid ECs, and poorly defined in clear cell ECs. The purpose of this study was to evaluate the occurrence of SCNAs in clinically diagnosed clear cell ECs. Paired tumor-normal DNAs for 51 ECs were hybridized to Illumina Infinium HumanHap650Y or Human660W-Quad Beadchips. Copy number calls were made using the Hidden Markov Model based SNP-FASST2 segmentation algorithm within Nexus Copy Number software (v.6.1). High-level SCNAs were defined as gain of ≥5 copies or homozygous deletion, both <10Mb. GISTIC 1.0, in Nexus, was used to identify statistically significant SCNAs, corrected for multiple testing. One or more high-level SCNAs were detected in 50% of 6 clear cell ECs, 78.6% of 28 serous ECs, and 17.6% of 17 endometrioid ECs. A positive association was found between high-level SCNAs and *TP53* mutation across ECs (two-tailed p value<0.0001). Classifying tumors according to *POLE*, MSI, and *TP53* status yielded four molecular subgroups; copy number altered tumors were more frequent in the *TP53*-mutated subgroup (95.8%) than in the unspecified subgroup (22.2%), and absent from the *POLE* and MSI subgroups. In conclusion, our study provides evidence of inter-tumor heterogeneity in the extent to which SCNAs occur in clinically diagnosed clear cell EC, and across molecular subgroups of EC. The co-occurrence of high-level SCNAs and *TP53* mutations in some clear cell ECs is consistent with the view that a subset of clinically diagnosed clear cell ECs have molecular similarities to serous ECs.

Keywords

Endometrial; uterine; cancer; clear cell; copy number

Corresponding Author: Dr. Daphne W. Bell, National Human Genome Research Institute, Cancer Genetics and Comparative Genomics Branch, 50 South Drive, MSC-8000, Bethesda, MD 20892; Phone (301) 594-9256; Fax (301) 594-1360; belldaph@mail.nih.gov.

AUTHOR CONTRIBUTIONS

Study conception (DWB), DNA isolation and purification (MLR), data analysis (AOH, MLG, MLR), manuscript preparation (DWB); edits and comments on the manuscript (AOH, MLG, MLR).

Declaration of interest: Dr. Daphne W. Bell receives royalty income from the licensing of US patent No. 7,294,468 "Method to determine responsiveness of cancer to epidermal growth factor receptor targeting treatments"

INTRODUCTION

Cancers of the uterine corpus are estimated to account for 11,350 deaths among American women in 2018 [1]. Endometrial carcinomas (ECs) make up the majority of uterine corpus tumors (reviewed in [2]) and are classified into a number of histopathologic subtypes including endometrioid, serous, and clear cell ECs. Endometrioid tumors constitute approximately 87–90% of newly diagnosed ECs, whereas serous and clear cell tumors, which by definition are high-grade tumors, account for approximately 3–10% and 1–3% of such cases [2, 3]. Compared with endometrioid ECs, serous and clear cell tumors have generally less favorable outcomes. For example, within the SEER registry (1988–2001), five-year relative survival rates were 91.2% for endometrioid, 44.7% for serous, and 64.8% for clear cell ECs [4], considering all stages and grades. For all histologies, increasing stage is associated with decreased outcomes [5, 6]. For endometrioid ECs, increasing grade is also associated with reduced outcomes [5, 6]. This fact is illustrated by a 5-year disease-specific survival rate of only 77% for grade 3-endometrioid ECs (all stages) within a study of cases in the SEER database [7], and by 5-year overall survival rates for grade 3 endometrioid EC ranging from 77.5% at stage I to 49.6% at stage III for cases within the National Cancer Database [6].

Endometrioid and serous ECs have been relatively well-studied at the molecular level (reviewed in [8, 9]), and were the focus of an integrated genomic analysis by The Cancer Genome Atlas (TCGA) [10]. They exhibit a number of differences in their molecular pathogenesis. The endometrioid subtype is typified by frequent aberrations in the PI3K-AKT-mTOR pathway, the WNT/β-catenin pathway, the RAS-RAF-MAPK-ERK pathway, and *ARID1A*, as well as frequent microsatellite instability (MSI) and relatively frequent somatic mutations affecting the exonuclease domain of *POLE* (reviewed in [11]). In contrast to endometrioid EC, serous EC frequently exhibits *TP53* mutation and/or p53 stabilization, *PPP2R1A* mutation, *ERBB2* amplification, and high-level somatic copy number alterations (SCNAs) (Reviewed in [12]).

The mutational profiles of some clear cell tumors resemble those of either serous or endometrioid ECs [13–21]. However, the extent to which genome-wide SCNAs occur in this subtype remains poorly understood. Very few clear cell ECs have been karyotyped or analyzed by chromosomal comparative genomic hybridization (cCGH) [22–24]. Moreover, high-resolution SNP array based genome-wide copy number analysis has, to our knowledge, only been reported for two primary clear cell ECs both of which were relatively copy number quiet [25].

Here, we used high-density, SNP array analysis to determine the incidence of SCNAs in six clinically diagnosed clear cell ECs, and, for comparison on the same platform, 28 serous ECs and 17 endometrioid ECs. Focal high-level SCNAs were detected in 50% of clear cell ECs, compared with 78.6% of serous, and 17.6% of endometrioid ECs. Stratifying tumors into "TCGA-like" molecular subgroups, agnostic of histology, revealed a significant association between copy number alterations and *TP53* mutations.

MATERIALS AND METHODS

Clinical material

The NIH Office of Human Subjects Research Protection determined that the research using the specimens in this study was not "human subjects research" per the Common Rule (45 CFR 46) and was exempt from IRB review. Snap-frozen primary tumor tissues, matched non-tumor tissues, and corresponding hematoxylin and eosin (H&E)-stained tumor sections were acquired as de-identified material from the Cooperative Human Tissue Network (CHTN), which is funded by the National Cancer Institute. Matched tumor and normal DNAs for four cases were purchased from Oncomatrix Inc (San Marcos, CA). Tumor specimens were collected at surgical resection prior to treatment. A histological classification was rendered based upon the entire specimen at time of diagnosis; this classification is used herein. For fresh-frozen tumor specimens received from CHTN, a single gynecologic pathologist reviewed an H&E section of this tumor tissue to identify regions of high (>70%) neoplastic cellularity for macrodissection and DNA isolation. Matched normal samples were from uninvolved reproductive tissue (n=49), buffy coat (n=1), or whole blood (n=1).

DNA extraction

Genomic DNA was isolated from regions of macrodissected tissue comprised of >70% neoplastic cells, and from normal tissues, using the PUREGENE kit (Qiagen) as described elsewhere [16, 17]. DNA yield was quantified using the Qubit fluorometer (Invitrogen).

Identity testing

To confirm that tumor-normal pairs were derived from the same individual, paired DNAs were typed using the Coriell Identity Mapping kit (Coriell) as previously described [16]. Genotyping fragments were resolved on an ABI-3730*xl* DNA analyzer (Applied Biosystems) and scored using GeneMapper software.

SNP genotyping

Genomic DNA from each tumor and normal sample was hybridized either to an Illumina Infinium HumanHap650Y Genotyping BeadChip (660,919 probes) by the NHGRI Genomics Core, or to an Illumina Infinium Human660W-Quad BeadChip (657,367 probes) by the Johns Hopkins University SNP Center. Hybridizations, as well as quantification of signal intensities and allele calls, were performed according to standard procedures. SNP positions and downstream analyses were based on the hg18/NCBI Build 36 of the human genome.

SNP data were visualized and preprocessed using GenomeStudio (v2011.1) (Illumina Inc), including implementation of the updated cluster generation protocol for SNPs on the X chromosome. LogR intensity ratios and B allele frequencies for all probes were exported from GenomeStudio and imported into Nexus Copy Number™ software (v.6.1) (BioDiscovery). Within Nexus, a customized linear systematic probe correction was applied to correct for waviness in the data, and to exclude data from probes that were unique to either BeadChip; only data from the 549,242 probes present on both Beadchips was retained.

Next, for each tumor-normal pair, the datasets were re-centered to user-defined regions of balanced heterozygosity that had similar Log R ratios across multiple chromosomes within the tumor sample. The copy number changes reported herein represent a derivation from this baseline of balanced heterozygosity, but it should not be assumed that the baseline represents a diploid state.

Copy number calls and allelic status calls were made using the Hidden Markov Model based SNP-FASST2 segmentation algorithm within Nexus Copy Number™ (v.6.1). For data generated on the HumanHap650Y Genotyping BeadChip, settings used in the SNP-FASST2 segmentation algorithm included a significance threshold of 1.0E-6, a maximum contiguous probe spacing of 1000kb, a minimum of 5 probes per segment, a homozygous frequency threshold of 0.85, a homozygous value threshold of 0.8, a heterozygous imbalance threshold of 0.4, a minimum LOH length of 500kb, a high gain of 0.6, a gain of 0.18, a loss of −0.18 and a big loss of −1.0. For data generated on the Human660W-Quad BeadChip, the settings used in the SNP-FASST2 segmentation algorithm were identical to those for the HumanHap650Y Genotyping BeadChip with the exception of the high gain and gain which were set at 0.38 and 0.1 respectively. We also used a setting of 3% for the removal of outliers in the Nexus calculation of probe-to-probe variance, or quality. Tumor-normal pairs for which the tumor and/or normal data had a Nexus quality score >0.1 after removing the top and bottom 1.5% of outlier probes, were considered to have poor quality data and were excluded from further analysis. Copy number alterations of the same type and at the same loci in tumor-normal pairs, were considered germline, and were manually removed from each tumor profile. Only somatic copy number alterations (SCNAs) were considered in subsequent analyses. We defined "focal high-level SCNAs" as gains of ≥5 copies or homozygous deletions, both <10Mb. Genomic co-ordinates of "high-level SCNAs" were converted from hg18 to hg19 using the UCSC LiftOver utility, and queried against "gold standard variants" in the Database of Genomic Variants (DGV) (URL:http://dgv.tcag.ca/dgv/app/home); regions that had at least 75% overlap with one or more "DGV Gold" variants were filtered out.

Regions of statistically significant copy number alteration (Q-bound value <= 0.25 and G-score cut-off ≥1.0) were identified within Nexus Copy Number (v.6.1) using GISTIC (Genomic Identification of Significant Targets in Cancer) 1.0 [26, 27]. Extended GISTIC regions of statistically significant SCNA and corresponding peak GISTIC regions were identified separately for tumor and normal datasets. Extended and peak regions present in both the combined tumor and combined normal datasets were manually excluded because they may represent germline CNVs. Extended and peak GISTIC regions that had at least 75% overlap with one or more "DGV Gold" variants were filtered out. Cancer genes in peak GISTIC regions were annotated by querying the Cancer Gene Census (COSMICv90) (URL: http://cancer.sanger.ac.uk/census/).

RESULTS

Somatic copy number status varies according to EC histotypes

We detected one or more SCNAs in 50.0% (3 of 6) of clear cell, 82.1% (23 of 28) serous, and 70.5% (12 of 17) of endometrioid ECs (Figure 1, Figure 2, Figure 3). Gains involving

3q, 5p, 8q, 20q, and 22q were the most frequent SCNAs amongst clear cell tumors (Figure 1, Supplementary Figure 1). In serous tumors, SCNAs occurred throughout the genome with gains often involving chromosomes 1p, 1q, 2p, 2q, 3q, 5p, 6p, 6q, 8q, 10p, 12p, 14q, 17q, 18p, 19q, 20p, and 20q, and losses affecting 4q, 7q, 8p, 9q, 15q, 16q, and 22q (Figure 2, Supplementary Figure 2). Gains involving chromosomes 1q, 3q, 7p, 8p, 8q, 10p, 10q, and losses involving 13q and 16q were the most common SCNAs among endometrioid ECs (Figure 3, Supplementary Figure 3). One or more focal high-level SCNAs were detected in 50% (3 of 6) of clear cell, 78.5% (22 of 28) of serous, and 17.6% (3 of 17) of endometrioid ECs (Supplementary Table 1, Supplementary Table 2, Supplementary Table 3, Supplementary Table 4). Consensus cancer genes residing within focal high-level SCNAs in clear cell EC included *KAT6B* (within a chr10q22.2-q22.3 gain in T28) and *MECOM* (within a chr3q26.1-q26.31 gain in T153) (Supplementary Table 2). Five genes (*ERBB2*, *CDK12*, *FGFR1*, *INPP4A*, and *PRKAR1A*) within focal high-level SCNAs in a clear cell EC (T153), have also been reported, via next generation sequencing, to be amplified among clear cell ECs [28].

Statistically significant SCNAs identified by GISTIC 1.0 analysis in histological subtypes of EC

GISTIC analysis identified one peak region of SCNA, involving chr4q34.3 loss, in clear cell EC (Supplementary Table 1); this region was devoid of protein-encoding genes but encompassed a long non-coding RNA gene (*LINC02500*) (Table 1). In contrast, there were 41 peak GISTIC regions of SCNA among serous tumors (Table 2). Genes in individual high level SCNAs in clear cell EC, and within GISTIC peaks in serous EC were *KAT6B*, *MECOM-ACTRT3-MYNN-LRRC34-LRR1Q4*, *ZMAT4*, *LINC02548-LINC02545*, *RNU6–2*; *LINC02082* was located within an individual high level SCNA in clear cell EC and in an endometrioid EC GISTIC peak. Consensus cancer genes in peak regions of serous EC GISTIC gain were *MECOM*, and *KAT6B*. Consensus cancer genes in peak regions of GISTIC loss in serous EC were *LRP1B*, *MAP2K4*, *ERBB4*, and *PTEN*. Eighteen protein-encoding genes in peak GISTIC regions in our serous ECs were also located in peak GISTIC regions in serous ECs and/or copy number cluster 4 ECs in TCGA [10] (Table 1, Table 2). Genes (and chromosomal locations) identified by both studies in peak GISTIC gains were *EVI1*/*MECOM*/*MDS1* and *MYNN* (both 3q26.2); *TERC* (3q26.2); *NEDD9* (6p24.2); *ZMAT4* (8p11.21); *PSD4* (2q13); and *KAT6B* (10q22.2). Genes identified by both studies in regions of peak GISTIC loss were *LRP1B* (2q22.1-q22.2); *WASF2* (1p36.11); *PTEN* (10q23.31); *AHDC1* (1p36.11-p35.3); *PDE4D* (5q11.2-q12.1); *DNAH9*, *MAP2K4*, and *ZNF18* (all 17p12); *ARAP2* (4p14); *TUSC1* (9p21.2); and *LHX1* and *AATF* (both 17q12). Several of these genes are proposed driver genes in statistically significant recurring SCNAs in the TCGA Pan-Gyn cohort specifically: *MECOM*, *NEDD9*, and *KAT6B* in GISTIC gains; *LRP1B*, *PDE4D*, *PTEN*, and *MAP2K4* in GISTIC losses [29].

To determine whether SCNA of genes in peak GISTIC regions in our serous EC cohort is associated with survival, we queried these genes in the TCGA serous EC (n=108) data [29], using the cBIOPortal [30, 31]. This analysis showed that *LAMC1* gain was statistically significantly associated with decreased overall survival (OS) (median OS 14.7 months *versus* 106.9 months; Logrank Test P-value 5.659e-4) and shorter disease-free survival

(DFS) (median disease-free interval 14.0 months *versus* NA; Logrank Test P-value 1.244e-4) for serous EC patients (Supplementary Figure 4). *SPIN4* gain was statistically significantly associated with reduced OS (Logrank Test P-value 2.828e-3) (Supplementary Figure 4), although this finding is based on a single patient with amplification.

GISTIC analysis of endometrioid ECs identified six significant peak regions of gain and one significant peak region of loss (Table 3). The consensus cancer gene *MRTFA*/*MKL1* was located within a peak region of GISTIC loss among endometrioid ECs. There was no overlap between the genes located in peak GISTIC regions in endometrioid ECs in this study and those in TCGA EC copy number cluster-2 or cluster-3, which were predominated by endometrioid ECs [10]. *ZMAT4 (Zinc finger matrin type 4)* was located within a peak region of gain in both serous and endometrioid ECs.

Correlation of SCNA status with *TP53* mutational status, MSI, and *POLE* mutational status

We previously reported the incidence of *TP53* somatic mutations (all coding exons) and microsatellite instability (MSI) for the 51 tumors in this study [18, 19]. Here, we compared the SCNA status and *TP53* status of tumors (Supplementary Table 5). We observed a statistically significant positive correlation between *TP53* mutation and the presence of focal high-level SCNAs across ECs: 85.7% (24 of 28) of tumors with focal high-level SCNAs were *TP53*-mutated compared with 4.3% (1 of 23) of tumors without focal high-level SCNAs (two-tailed p value<0.0001). With respect to histologic subtype, all (3 of 3) clear cell tumors with focal high-level SCNAs were *TP53*-mutated versus 0% (0 of 3) of clear cell tumors without focal high-level SCNAs, a difference that was not statistically significant; 90.9% (20 of 22) of serous tumors with focal high-level SCNAs were *TP53*-mutated compared with 0% (0 of 6) of serous tumors without focal high-level SCNAs (two-tailed p value<0.0001); and 33.3% (1 of 3) of endometrioid tumors with focal high-level SCNAs were *TP53*-mutated versus 7.1% (1 of 14) of tumors without focal high-level SCNAs, a difference that was not statistically significant.

No statistically significant associations were found between the presence of focal high-level SCNAs and MSI in any histotype. MSI was not detected in any clear cell or serous ECs in this study. For endometrioid ECs, 0% (0 of 3) of tumors with focal high-level SCNAs had MSI compared with 28.6% (4 of 14) of tumors without high-level SCNAs, a difference that was not statistically significant.

The *POLE* (exon 3–13) mutation status of 49 tumors in this study was reported elsewhere [32]. *POLE* hotspot mutations (Supplementary Table 5) were present in one endometrioid EC, and in two of eight (25%) *TP53* wildtype serous tumors versus 0 of 20 (0%) *TP53* mutant serous tumors (a difference that was not statistically significant) (Supplementary Table 5). Focal high-level SCNAs were not detected in either of the *POLE*-mutated tumors or in MSI tumors.

Distribution of SCNAs and GISTIC regions in "TCGA-like" molecular subtypes of EC

MSI status, the mutational status of the *POLE* exonuclease domain (ED)(exons 9–13), and the mutational status of *TP53* can be used to approximate the TCGA molecular subtypes of EC [33]. We therefore stratified the 49 tumors previously typed for all three markers into the

following molecular groups: *POLE*-ED-mutated (n=3), MSI (n=4), *TP53*-mutated (n=24), and unspecified (MSS/POLE-ED-wildtype/*TP53*-wildtype) (n=18) (Supplementary Table 5). Tumors with any level of SCNA were more common in the *TP53*-mutated group (100%, 24 of 24) than in the unspecified group (50%, 9 of 18) and were absent from the *POLE*-mutated (0 of 3) and MSI-high (0 of 4) groups. Tumors with focal high-level SCNAs (gains of ≥5 copies or homozygous deletions, both <10Mb) were more frequent in the *TP53*-mutated group (95.8%, 23 of 24) than in the unspecified group (22.2%, 4 of 18), a difference that was statistically significant (two-tailed p value<0.0001). No GISTIC regions of SCNA were detected in the *POLE*-ED-mutated or MSI groups whereas the *TP53*-mutated and unspecified groups had 41 and 8 GISTIC regions of SCNA respectively (Table 4 and Table 5). Among tumors within the *TP53*-mutated group, consensus cancer genes *KAT6B*, *MECOM*, *ERBB2*, *PTEN* and *LRP1B* were within peak GISTIC regions (Table 4). No consensus cancer genes were identified among tumors within the unspecified molecular subgroup (Table 5).

DISCUSSION

Clear cell EC is a rare histological subtype of uterine cancer that is associated with relatively poor clinical outcomes [4, 34] and to date is lacking the genomic characterization to which other EC histologic subtypes have been subjected. Here we provide high-resolution copy number analysis of 6 clinically diagnosed clear cell ECs and show that half of these tumors have acquired one or more SCNAs; the most frequent SCNAs involved gains of 3q, 5p, 8q, 20q, and 22q. Our findings are consistent with a comparative genomic hybridization (CGH) study by Micci et al., which reported genomic imbalances in 75% (3 of 4) of clear cell ECs, with gains involving 3q and 8q occurring in all chromosomally unstable tumors [23]. Compared to gains, we found that genomic losses in copy number altered clear cell ECs were relatively rare, which is also consistent with previous observations [23]. Although we observed no statistically significant association between *TP53* mutation status and copy number status in clear cell EC, it is noteworthy that *TP53* mutations were restricted to tumors with focal high-level SCNAs.

By comparison to clear cell ECs, 82.1% of serous and 70.5% of endometrioid ECs in our study had at least one SCNA. The fraction of tumors with focal high-level SCNAs was greater for serous than endometrioid ECs (78.6% versus 17.6% respectively). Our observations that SCNAs in serous tumors were widely distributed throughout the genome and consisted of gains and losses, whereas SCNAs in endometrioid tumors often involved chromosomes 1, 3, 7, 8 and 10 and tended to be gains, is in keeping with the distribution of SCNAs observed by TCGA in these histotypes [10] and in an early CGH study by Pere et al [35].

We noted a positive correlation between *TP53* mutation and the presence of focal high-level SCNA in ECs (two-tailed p value<0.0001). Although the overall frequency of *TP53* mutations in our serous EC cohort (71%) is relatively low, it is within the range (59%-93%, mean 81.7%) reported by others [10, 28, 36–40]. Inter-study variability in *TP53* mutation rate may reflect differences in the extent of pathological review of tumors; studies based on clinical diagnoses, such as ours, will inevitably reflect the challenges in reliably determining

the histology of some high-grade endometrial tumors [41]. Because of the well-known challenges associated with reproducible histopathologic diagnoses of a subset of ECs [42], we stratified our entire tumor cohort into "TCGA-like" molecular subgroups based on *POLE* (exonuclease domain) mutation status, MSI status, and *TP53* mutation status. Clear cell ECs were equally distributed among the *TP53* mutated and unspecified groups. Copy number altered tumors were more common in the *TP53*-mutated group than in the unspecified group and were absent from the *POLE*-mutated or MSI-high groups. The most statistically significant peak GISTIC regions in the *TP53*-mutated group were gains involving 3q26.2 (*MECOM, ACTRT3, MYNN, LRRC34, LRRIQ4, TERC*), 19q12-q13.11 (*PLEKHF1*, *C19orf12*), and 20q13.2. Although the peak GISTIC region on 20q13.2 did not encompass any gene, the corresponding extended GISTIC region included *ZNF217*, a putative oncogene that is amplified and/or overexpressed in a variety of tumor types [43]. Of note, *MECOM*, *TERC*, and *ZNF217* are also in significantly recurring regions of amplification in TCGA copy number cluster 4 tumors. Other genes in peak GISTIC regions in the *TP53*-mutated group and in significantly recurring regions of SCNA in TCGA copy number cluster 4 tumors are *NEDD9*, *ERBB2*, and *LRP1B*.

While our study provides insights into the occurrence of SCNAs in clear cell ECs, it has several limitations. Our analysis was restricted to a small number of clinically diagnosed clear cell ECs. Because clear cell ECs and a subset of serous ECs are recognized as being difficult to reproducibly classify, even by multiple gynecologic pathologists [41, 44–48], our findings should be viewed in the context of clinically diagnosed cases, not consensus (pure) cases. As such, our study was not designed to reliably evaluate certain genotype-phenotype correlations such as the issue of whether *TP53*-mutant clear cell ECs are really serous carcinomas with clear cell-like morphology. Studies to address such questions are important future directions for the field. Finally, in the absence of orthogonal validation, the copy number alterations reported herein should be regarded as putative alterations.

In conclusion, using high resolution SNP-based array analysis, we show that some clinically diagnosed clear cell ECs have high-level copy number alterations and are *TP53*-mutated whereas others are relatively copy number quiet and *TP53*-nonmutated, a finding that corroborates previous reports of genomic heterogeneity in clear cell ECs with respect to mutations [13–21]. Our observations that SCNAs are more frequent in serous EC than in low- and intermediate-grade endometrioid ECs also confirms previous observations [10]. To our knowledge this is only the second series of primary clear cell ECs analyzed genome-wide for somatic copy number alterations using high-resolution SNP arrays. Our findings add to the current understanding of the molecular etiology of this rare but often clinically aggressive histological subtype of EC and provide impetus for future studies.

Supplementary Material

Refer to Web version on PubMed Central for supplementary material.

ACKNOWLEDGEMENTS

Our sincere thanks to Dr. Mary Ellen Urick for critical and insightful comments on the manuscript. We thank Settara Chandrasekharappa, Ph.D., MaryPat Sussex Jones, M.S., and Ursula Harper M.S., of the NHGRI Genomics

Core, and Kim Doheny, Ph.D., Roxann Ashworth, M.H.S., and Michelle Zilka, M.S., at the Center for Inherited Disease Research (CIDR) at Johns Hopkins University for technical assistance. Data have been deposited into dbGaP (phs001690.v1.p1) with controlled-access.

FUNDING

This work was supported by the Intramural Research Program of the National Human Genome Research Institute, National Institutes of Health.

REFERENCES

[1]. American Cancer Society. Cancer Facts and Figures. American Cancer Society 2018;1:1–76.

[2]. Dedes KJ, Wetterskog D, Ashworth A, Kaye SB, Reis-Filho JS. Emerging therapeutic targets in endometrial cancer. Nat Rev Clin Oncol 2011;8:261–71. [PubMed: 21221135]

[3]. Clement PB, Young RH. Non-endometrioid carcinomas of the uterine corpus: a review of their pathology with emphasis on recent advances and problematic aspects. Adv Anat Pathol 2004;11:117–42. [PubMed: 15096727]

[4]. Ries LAG, Young JL, Keel GE, Eisner MP, Lin YD, Horner M-J. SEER Survival Monograph: Cancer Survival Among Adults: U.S. SEER Program, 1988–2001 Patient and tumor characteristics. National Cancer Institute, SEER Program, NIH Pub No 07–6215, Bethesda, MD, 2007.

[5]. Creasman WT, Odicino F, Maisonneuve P, Quinn MA, Beller U, Benedet JL, et al. Carcinoma of the corpus uteri. FIGO 26th annual report on the results of treatment in gynecological cancer. Int J Gynaecol Obstet 2006;95 Suppl 1:S105–43.

[6]. McGunigal M, Liu J, Kalir T, Chadha M, Gupta V. Survival differences among uterine papillary serous, clear cell and grade 3 endometrioid adenocarcinoma endometrial cancers: a national cancer database analysis. Int J Gynecol Cancer 2017;27:85–92. [PubMed: 27759595]

[7]. Hamilton CA, Cheung MK, Osann K, Chen L, Teng NN, Longacre TA, et al. Uterine papillary serous and clear cell carcinomas predict for poorer survival compared to grade 3 endometrioid corpus cancers. Br J Cancer 2006;94:642–6. [PubMed: 16495918]

[8]. Walker CJ, Goodfellow PJ. Traditional approaches to molecular genetic analysis. Adv Exp Med Biol 2017;943:99–118. [PubMed: 27910066]

[9]. Le Gallo M, Lozy F, Bell DW. Next-generation sequencing. Adv Exp Med Biol 2017;943:119–48. [PubMed: 27910067]

[10]. Kandoth C, Schultz N, Cherniack AD, Akbani R, Liu Y, Shen H, et al. Integrated genomic characterization of endometrial carcinoma. Nature 2013;497:67–73. [PubMed: 23636398]

[11]. Murali R, Soslow RA, Weigelt B. Classification of endometrial carcinoma: more than two types. Lancet Oncol 2014;15:e268–78. [PubMed: 24872110]

[12]. Urick ME, Rudd ML, Bell DW. Molecular pathology of serous carcinoma In: Deavers MT, Coffey D, editors. Precision molecular pathology of uterine cancer: Springer, 2017;87–122.

[13]. An HJ, Logani S, Isacson C, Ellenson LH. Molecular characterization of uterine clear cell carcinoma. Mod Pathol 2004;17:530–7. [PubMed: 14976538]

[14]. Huang HN, Chiang YC, Cheng WF, Chen CA, Lin MC, Kuo KT. Molecular alterations in endometrial and ovarian clear cell carcinomas: clinical impacts of telomerase reverse transcriptase promoter mutation. Mod Pathol 2015;28:303–11. [PubMed: 25081752]

[15]. Hoang LN, McConechy MK, Meng B, McIntyre JB, Ewanowich C, Gilks CB, et al. Targeted mutation analysis of endometrial clear cell carcinoma. Histopathology 2015;40:166–80.

[16]. Rudd ML, Price JC, Fogoros S, Godwin AK, Sgroi DC, Merino MJ, et al. A unique spectrum of somatic PIK3CA (p110alpha) mutations within primary endometrial carcinomas. Clin Cancer Res 2011;17:1331–40. [PubMed: 21266528]

[17]. Urick ME, Rudd ML, Godwin AK, Sgroi D, Merino M, Bell DW. PIK3R1 (p85alpha) is somatically mutated at high frequency in primary endometrial cancer. Cancer Res 2011;71:4061–7. [PubMed: 21478295]

[18]. Le Gallo M, O'Hara AJ, Rudd ML, Urick ME, Hansen NF, O'Neil NJ, et al. Exome sequencing of serous endometrial tumors identifies recurrent somatic mutations in chromatin-remodeling and ubiquitin ligase complex genes. Nat Genet 2012;44:1310–5. [PubMed: 23104009]

[19]. Le Gallo M, Rudd ML, Urick ME, Hansen NF, Zhang S, NISC Comparative Sequencing Program, et al. Somatic mutation profiles of clear cell endometrial tumors revealed by whole exome and targeted gene sequencing. Cancer 2017;123:3261–8. [PubMed: 28485815]

[20]. DeLair DF, Burke KA, Selenica P, Lim RS, Scott SN, Middha S, et al. The genetic landscape of endometrial clear cell carcinomas. J Pathol 2017;243:230–31. [PubMed: 28718916]

[21]. Stelloo E, Bosse T, Nout RA, MacKay HJ, Church DN, Nijman HW, et al. Refining prognosis and identifying targetable pathways for high-risk endometrial cancer; a TransPORTEC initiative. Mod Pathol 2015;28:836–44. [PubMed: 25720322]

[22]. Suzuki A, Fukushige S, Nagase S, Ohuchi N, Satomi S, Horii A. Frequent gains on chromosome arms 1q and/or 8q in human endometrial cancer. Hum Genet 1997;100:629–36. [PubMed: 9341884]

[23]. Micci F, Teixeira MR, Haugom L, Kristensen G, Abeler VM, Heim S. Genomic aberrations in carcinomas of the uterine corpus. Genes Chromosomes Cancer 2004;40:229–46. [PubMed: 15139002]

[24]. Bardi G, Pandis N, Schousboe K, Holund B, Heim S. Near-diploid karyotypes with recurrent chromosome abnormalities characterize early-stage endometrial cancer. Cancer Genet Cytogenet 1995;80:110–4. [PubMed: 7736425]

[25]. Gibson WJ, Hoivik EA, Halle MK, Taylor-Weiner A, Cherniack AD, Berg A, et al. The genomic landscape and evolution of endometrial carcinoma progression and abdominopelvic metastasis. Nat Genet 2016;48:848–55 [PubMed: 27348297]

[26]. Beroukhim R, Getz G, Nghiemphu L, Barretina J, Hsueh T, Linhart D, et al. Assessing the significance of chromosomal aberrations in cancer: methodology and application to glioma. Proc Natl Acad Sci U S A 2007;104:20007–12. [PubMed: 18077431]

[27]. Petrini I, Meltzer PS, Kim IK, Lucchi M, Park KS, Fontanini G, et al. A specific missense mutation in GTF2I occurs at high frequency in thymic epithelial tumors. Nat Genet 2014;46:844–9 [PubMed: 24974848]

[28]. Soumerai TE, Donoghue MTA, Bandlamudi C, Srinivasan P, Chang MT, Zamarin D, et al. Clinical utility of prospective molecular characterization in advanced endometrial cancer. Clin Cancer Res 2018;24:5939–47. [PubMed: 30068706]

[29]. Berger AC, Korkut A, Kanchi RS, Hegde AM, Lenoir W, Liu W, et al. A comprehensive pan-cancer molecular study of gynecologic and breast cancers. Cancer Cell 2018;33:690–705. [PubMed: 29622464]

[30]. Cerami E, Gao J, Dogrusoz U, Gross BE, Sumer SO, Aksoy BA, et al. The cBio cancer genomics portal: an open platform for exploring multidimensional cancer genomics data. Cancer Discov 2012;2:401–4. [PubMed: 22588877]

[31]. Gao J, Aksoy BA, Dogrusoz U, Dresdner G, Gross B, Sumer SO, et al. Integrative analysis of complex cancer genomics and clinical profiles using the cBioPortal. Sci Signal 2013;6:pl1. [PubMed: 23550210]

[32]. Rudd ML, Mohamed H, Price JC, O'Hara AJ, Le Gallo M, Urick ME, et al. Mutational analysis of the tyrosine kinome in serous and clear cell endometrial cancer uncovers rare somatic mutations in TNK2 and DDR1. BMC Cancer 2014;14:884. [PubMed: 25427824]

[33]. Talhouk A, McConechy MK, Leung S, Yang W, Lum A, Senz J, et al. Confirmation of ProMisE: A simple, genomics-based clinical classifier for endometrial cancer. Cancer 2017;123:802–13. [PubMed: 28061006]

[34]. Hasegawa K, Nagao S, Yasuda M, Millan D, Viswanathan AN, Glasspool RM, et al. Gynecologic Cancer InterGroup (GCIG) consensus review for clear cell carcinoma of the uterine corpus and cervix. Int J Gynecol Cancer 2014;24:S90–5. [PubMed: 25341588]

[35]. Pere H, Tapper J, Wahlstrom T, Knuutila S, Butzow R. Distinct chromosomal imbalances in uterine serous and endometrioid carcinomas. Cancer Res 1998;58:892–5. [PubMed: 9500445]

[36]. Zhao S, Choi M, Overton JD, Bellone S, Roque DM, Cocco E, et al. Landscape of somatic single-nucleotide and copy-number mutations in uterine serous carcinoma. Proc Natl Acad Sci U.S.A. 2013;110:2916–2. [PubMed: 23359684]

[37]. McConechy MK, Ding J, Cheang MC, Wiegand K, Senz J, Tone A, et al. Use of mutation profiles to refine the classification of endometrial carcinomas. J Pathol 2012;228:20–30. [PubMed: 22653804]

[38]. Kuhn E, Wu RC, Guan B, Wu G, Zhang J, Wang Y, et al. Identification of molecular pathway aberrations in uterine serous carcinoma by genome-wide analyses. J Natl Cancer Inst 2012;104:1503–13. [PubMed: 22923510]

[39]. Tashiro H, Isacson C, Levine R, Kurman RJ, Cho KR, Hedrick L. p53 gene mutations are common in uterine serous carcinoma and occur early in their pathogenesis. Am J Pathol 1997;150:177–85. [PubMed: 9006334]

[40]. Lax SF, Kendall B, Tashiro H, Slebos RJ, Hedrick L. The frequency of p53, K-ras mutations, and microsatellite instability differs in uterine endometrioid and serous carcinoma: evidence of distinct molecular genetic pathways. Cancer 2000;88:814–24. [PubMed: 10679651]

[41]. Gilks CB, Oliva E, Soslow RA. Poor interobserver reproducibility in the diagnosis of high-grade endometrial carcinoma. Am J Surg Pathol 2013;37:874–81. [PubMed: 23629444]

[42]. Murali R, Davidson B, Fadare O, Carlson JA, Crum CP, Gilks CB, et al. High-grade endometrial carcinomas: morphologic and immunohistochemical features, diagnostic challenges and recommendations. Int J Gynecol Pathol 2019;38 Suppl 1:S40–S63. [PubMed: 30550483]

[43]. Rahman MT, Nakayama K, Rahman M, Nakayama N, Ishikawa M, Katagiri A, et al. Prognostic and therapeutic impact of the chromosome 20q13.2 ZNF217 locus amplification in ovarian clear cell carcinoma. Cancer 2012;118:2846–57. [PubMed: 22139760]

[44]. Thomas S, Hussein Y, Bandyopadhyay S, Cote M, Hassan O, Abdulfatah E, et al. Interobserver variability in the diagnosis of uterine high-grade endometrioid carcinoma. Arch Pathol Lab Med 2016;140:836–43. [PubMed: 27139150]

[45]. Han G, Soslow RA, Wethington S, Levine DA, Bogomolniy F, Clement P, et al. Endometrial carcinomas with clear cells: a study of a heterogeneous group of tumors including interobserver variability, mutation analysis, and immunohistochemistry with HNF-1beta. Int J Gynecol Pathol 2015;34:323–33. [PubMed: 25851704]

[46]. Fadare O, Parkash V, Dupont WD, Acs G, Atkins KA, Irving JA, et al. The diagnosis of endometrial carcinomas with clear cells by gynecologic pathologists: an assessment of interobserver variability and associated morphologic features. Am J Surg Pathol 2012;36:1107–18. [PubMed: 22790851]

[47]. Han G, Sidhu D, Duggan MA, Arseneau J, Cesari M, Clement PB, et al. Reproducibility of histological cell type in high-grade endometrial carcinoma. Mod Pathol 2013;26:1594–604. [PubMed: 23807777]

[48]. Clarke BA, Gilks CB. Endometrial carcinoma: controversies in histopathological assessment of grade and tumour cell type. J Clin Pathol 2010;63:410–5. [PubMed: 20418232]

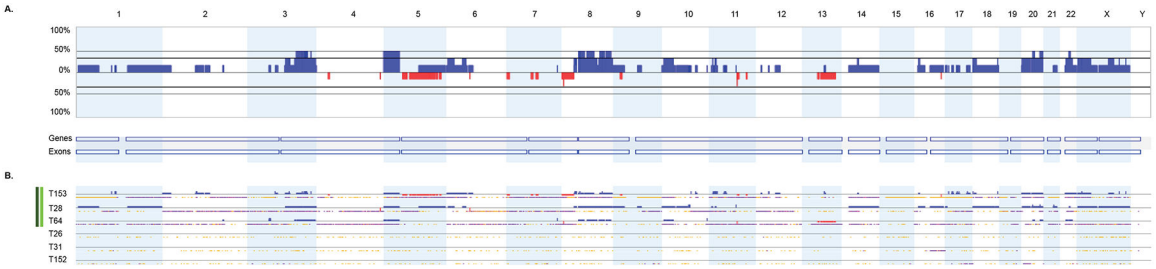

Figure 1.

Distribution of SCNAs among six clear cell ECs. (**A**) Genome-wide frequency plots of SCNAs for all cases combined. The frequency plot shows the percentage of tumors with somatic copy number gains (dark blue) and losses (red) above and below baseline (0%). (**B**) Profiles of SCNAs within each individual tumor (T). Tumors with at least one SCNA are indicated by the dark green column (left); tumors with at least one focal high-level SCNA are indicated by the light green column (left). Chromosomes 1 through 22 and the sex chromosomes are displayed sequentially from left to right.

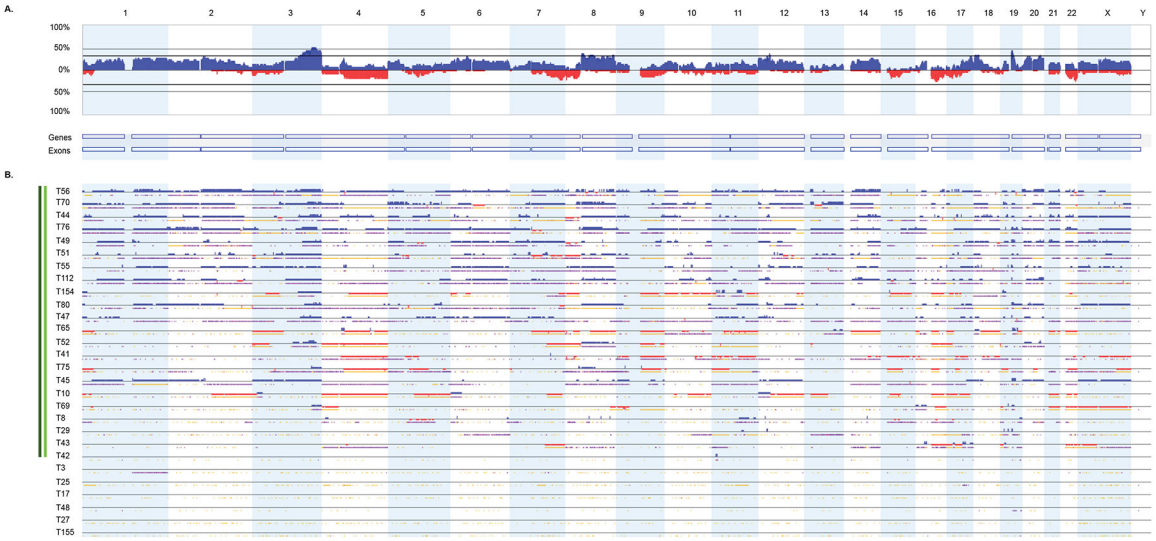

Figure 2.

Distribution of SCNAs among 28 serous ECs. (**A**) Genome-wide frequency plots of SCNAs for all cases combined. The frequency plot shows the percentage of tumors with somatic copy number gains (dark blue) and losses (red) above and below baseline (0%). (**B**) Profiles of SCNAs within each individual tumor (T). Tumors with at least one SCNA are indicated by the dark green column (left); tumors with at least one focal high-level SCNA are indicated by the light green column (left). Chromosomes 1 through 22 and the sex chromosomes are displayed sequentially from left to right.

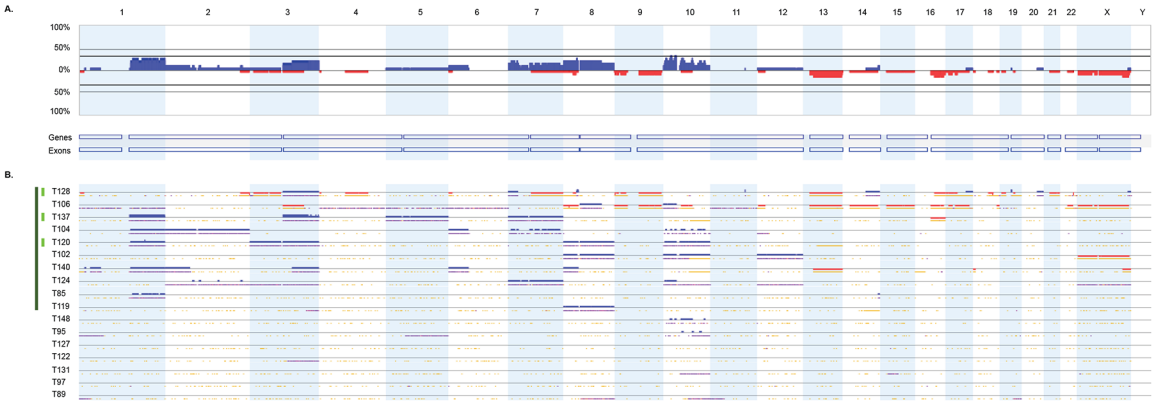

Figure 3.

Distribution of SCNAs among 17 endometrioid ECs. (**A**) Genome-wide frequency plots of SCNAs for all cases combined. The frequency plot shows the percentage of tumors with somatic copy number gains (dark blue) and losses (red) above and below baseline (0%). (**B**) Profiles of SCNAs within each individual tumor (T). Tumors with at least one SCNA are indicated by the dark green column (left); tumors with at least one focal high-level SCNA are indicated by the light green column (left). Chromosomes 1 through 22 and the sex chromosomes are displayed sequentially from left to right.

Table 1.

Extended and peak GISTIC regions identified among clear cell ECs

SCNA Type	Genomic Coordinates (hg18) of Extended GISTIC Region	Chromosomal Location of Extended GISTIC Region	Genomic Coordinates (hg18) of Peak GISTIC Region	Q-bound for Peak Region	G-Score for Peak Region	Genes in Peak GISTIC Region
Loss	chr4:97,886,832-191,273,063		chr4:182,415,084-182,433,256	0.24887827	1.17969014	*LINC02500*

Table 2.

Extended and peak GISTIC regions identified among serous ECs

SCNA Type	Genomic Coordinates (hg18) of Extended GISTIC Region	Chromosomal Location of Extended GISTIC Region	Genomic Coordinates (hg18) of Peak GISTIC Region	Q-bound for Peak Region	G-Score for Peak Region	Genes in Peak GISTIC Region
Gain	chr1:176,942,142-190,068,868	1q25.2-q31.2	chr1:181,211,397-181,376,609	5.04E-3	4.568	*LAMC1, LAMC1-AS1*
Gain	chr1:42,689,950-49,840,316	1p34.2-p33	chr1:44,358,961-44,455,683	7.26E-2	3.842	*KLF17, DMAP1*
Gain	chr10:76,048,493-86,655,854	10q22.2-q23.1	chr10:76,285,006-76,292,848	8.97E-2	3.789	***KAT6B (MYST4)***^
Gain	chr11:13,107,660-17,245,167	11p15.2-p15.1	chr11:13,807,145-13,855,429	1.72E-1	3.553	*LINC02548, LINC02545*
Gain	chr12:24,710,025-25,457,711	12p12.1	chr12:24,983,158-25,022,328	6.31E-05	5.447	*BCAT1*
Gain	chr13:91,908,665-92,569,702	13q31.3	chr13:92,353,870-92,391,097	9.63E-2	3.764	/
Gain	chr14:42,169,974-85,498,415	14q21.2-31.3	chr14:45,216,232-45,273,870	9.97E-2	3.757	*LINC02303*
Gain	chr16:29,245,504-32,045,466	16p11.2	chr16:30,279,779-30,400,867	1.20E-1	3.681	*TBC1D10B, MYLPF, SEPTIN1, ZNF48, ZNF771, DCTPP1, SEPHS2, ITGAL, SNORA80C*
Gain	chr18:4,158,565-16,100,000	18p11.31-p11.1	chr18:10,911,569-11,090,060	1.49E-2	4.287	*PIEZO2*
Gain	chr19:22,755,564-24,191,440	19p12	chr19:22,831,403-22,857,036	2.56E-3	4.717	*ZNF723*
Gain	chr19:34,477,100-37,581,903	19q12-q13.11	chr19:34,839,864-34,892,756	5.73E-14	10.488	*PLEKHF1, C19orf12*
Gain	chr2:94,793,151-118,939,207	2q11.1-q14.2	chr2:113,590,192-113,656,137	2.69E-2	4.124	*IL1RN, PSD4*^
Gain	chr20:14,929,825-17,414,153	20p12.1	chr20:15,505,853-15,529,115	9.40E-3	4.408	*MACROD2*
Gain	chr20:51,602,600-51,797,590	20q13.2	chr20:51,722,390-51,726,725	9.44E-08	6.587	/
Gain	chr21:28,466,487-46,944,323	21q21.3-q22.3	chr21:43,661,758-43,750,095	1.40E-1	3.632	*SIK1, SIK1B, LINC00319, LINC01669*
Gain	chr3:169,808,488-171,669,472	3q26.2	chr3:170,858,670-171,032,269	4.45E-11	7.895	***MECOM***^, *ACTRT3, MYNN*^, *LRRC34, LRRIQ4, TERC* **
Gain	chr4:61,820,279-64,360,471	4q13.1	chr4:64,148,793-64,360,471	1.54E-2	4.275	/
Gain	chr6:11,306,574-11,952,750	6p24.1	chr6:11,470,627-11,545,036	1.53E-3	4.823	*NEDD9*^
Gain	chr7:37,375,580-57,890,326	7p14.2-p11.1	chr7:53,114,918-53,194,448	3.20E-2	4.070	/
Gain	chr8:129,370,592-132,726,767	8q24.21-q24.22	chr8:129,601,251-129,636,803	1.49E-2	4.283	*LINC00824*
Gain	chr8:40,154,687-43,910,848	8p11.21-p11.1	chr8:40,583,025-40,670,377	1.94E-2	4.214	*ZMAT4***
Gain	chrX:61,845,481-69,098,104	Xq11.1-q13.1	chrX:61,845,481-62,571,001	2.01E-1	3.495	*SPIN4, LINC01278*
Loss	chr1:16,797,436-35,789,123	1p36.13-p34.3	chr1:27,616,247-27,756,094	6.82E-2	4.597	*WASF2*^, *AHDC1*^
Loss	chr10:89,251,828-90,869,249	10q23.2-q23.31	chr10:89,620,956-89,745,318	9.04E-2	2.421	***PTEN****
Loss	chr16:33,744,011-34,319,481	16p11.2	chr16:33,744,011-34,311,321	6.82E-2	3.473	*LOC112268173, MIR9901*

SCNA Type	Genomic Coordinates (hg18) of Extended GISTIC Region	Chromosomal Location of Extended GISTIC Region	Genomic Coordinates (hg18) of Peak GISTIC Region	Q-bound for Peak Region	G-Score for Peak Region	Genes in Peak GISTIC Region
Loss	chr16:45,079,464-45,425,095	16q11.2	chr16:45,096,893-45,329,968	6.82E-2	3.188	*SHCBP1, VPS35,ORC6,MYLK3*
Loss	chr17:10,300,648-16,935,194	17p13.1-p11.2	chr17:11,807,637-11,917,951	6.82E-2	3.290	*DNAH9*^, *ZNF18*^,***MAP2K4***^
Loss	chr17:30,019,514-33,321,712	17q12	chr17:32,373,680-32,486,434	9.04E-2	2.426	*LHX1*^, *AATF*^, *MIR2909*
Loss	chr19:5,166,212-8,072,557	19p13.3-p13.2	chr19:7,120,029-7,174,340	1.80E-1	2.069	*INSR*
Loss	chr19:0-1,654,336	19p13-3	chr19:839,331-876,857	6.82E-2	5.197	*MED16, R3HDM4, KISS1R, RNU6-2*
Loss	chr2:141,290,607-142,091,845	2q22.1	chr2:141,514,130-141,549,533	6.82E-2	3.629	***LRP1B***^
Loss	chr2:212,586,754-213,027,807	2q34	chr2:212,761,893-212,772,982	8.48E-2	2.477	***ERBB4***
Loss	chr22:14,884,399-20,930,009	22q11.1-q11.22	chr22:15,869,733-15,915,743	1.72E-1	2.089	*CECR7*
Loss	chr22:45,341,436-49,691,432	22q13.31-q13.33	chr22:47,505,660-47,562,070	6.82E-2	3.612	*TAFA5*
Loss	chr4:115,451,731-140,666,120	4q26-q31.1	chr4:129,663,522-129,691,216	6.95E-2	2.722	/
Loss	chr4:181,771,427-182,320,436	4q34.3	chr4:182,084,359-182,181,085	6.82E-2	3.525	/
Loss	chr4:35,651,979-48,132,950	4p14-p12	chr4:35,780,455-35,831,233	6.82E-2	3.158	*ARAP2*^
Loss	chr5:56,081,575-63,823,550	5q11.2-q12.3	chr5:59,205,723-59,266,038	6.82E-2	3.602	*PDE4D*^
Loss	chr9:74,060,683-90,190,867	9q21.13-q22.1	chr9:80,427,442-80,485,053	6.90E-2	2.785	/
Loss	chrX: 121,101,286-121,546,546	Xq25	chrX: 121,162,142-121,262,032	6.82E-2	4.580	/

Consensus cancer genes (* Tier-1 or ** Tier 2; COSMIC v90) are shown in bold

*gene located in peak region in TCGA copy number cluster 4 [10]

**gene located in peak region in TCGA serous EC [10]

^genes located in peak region in TCGA copy number cluster 4 and serous EC [10]

Table 3.

Extended and peak GISTIC regions identified among endometrioid ECs

SCNA Type	Genomic Coordinates (hg18) of Extended GISTIC Region	Chromosomal Location of Extended GISTIC Region	Genomic Coordinates (hg18) of Peak GISTIC Region	Q-bound for Peak Region	G-Score for Peak Region	Genes in Peak GISTIC Region
Gain	chr1:147,305,744-247,249,719	1q21.1-q44	chr1:189,156,518-189,322,948	4.13E-03	1.669	/
Gain	chr10:11,552,951-30,309,068	10p14-p11.23	chr10:23,244,490-23,432,842	4.75E-02	1.099	*ARMC3*
Gain	chr10:41,756,307-45,536,421	10q11.1-q11.21	chr10:42,305,364-42,587,946	1.85E-02	1.194	*ZNF33B, LINC008039, LINC01518,LOC283028,LOC105378269*
Gain	chr3:121,385,071-192,547,654	3q13.33-q28	chr3:170,041,278-170,109,492	9.99E-02	1.255	*LINC02082*
Gain	chr7:109,318,773-109,646,296	7q31.1	chr7:109,318,773-109,412,379	7.37E-02	1.024	/
Gain	chr8:37,345,764-43,910,848	8p12-p11.1	chr8:40,608,933-40,638,501	5.90E-03	1.319	*ZMAT4*
Loss	chr22:14,884,399-49,691,432	22q11.1-q13.33	chr22:39,148,396-39,289,536	6.26E-02	1.875	***MRTFA/MKL1***
Loss	chrX:61,845,481-148,937,305	Xq11.1-q28	chrX:93,562,756-93,703,848	6.26E-03	1.001	*PLCXD1, GTPBP6, PPP2R3B, SHOX*

Consensus cancer genes (* Tier-1 or ** Tier 2; COSMIC v90) are shown in bold

Table 4.

Extended and peak GISTIC regions identified among the *TP53*-mutated molecular subgroup of EC

SCNA Type	Genomic Coordinates (hg18) of Extended GISTIC Region	Location of Extended GISTIC Region	Genomic Coordinates (hg18) of Peak GISTIC Region	Q-bound for Peak Region	G-Score for Peak Region	Genes in Peak GISTIC Region
Gain	chr1:114027311-121013322	1p13.2-p11.2	chr1:115921462-116005785	3.96E-2	4.374	*VANGL1*
Gain	chr1:176942142-207275546	1q25.2-q32.2	chr1:181211397-181376609	2.00E-3	5.110	*LAMC1*, *LAMC1-AS1*
Gain	chr10:76097779-76809750	10q22.2	chr10:76285006-76292848	3.32E-3	4.996	***KAT6B***
Gain	chr12:24710025-25457711	12p12.1	chr12:24983158-25022328	1.57E-4	5.674	*BCAT1*
Gain	chr13:91908665-92569702	13q31.3	chr13:92353870-92391097	2.25E-1	3.713	/
Gain	chr14:73019559-85498415	14q24.3-q31.3	chr14:73276000-73364208	2.60E-2	4.491	*ELMSAN1*, *MIR4505*, *LOC100506476*, *LINC02274*
Gain	chr17:34942209-35561769	17q12-q21.1	chr17:35024060-35199745	2.70E-2	4.482	*PPP1R1B*, *STARD3*, *TCAP*, *PNMT*, *PGAP3*, ***ERBB2***, *MIEN1*, *GRB7*, *IKZF3*, *MIR4728*
Gain	chr18:0-16100000	18p11.32-p11.1	chr18:10911569-11090060	1.37E-2	4.658	*PIEZO2*
Gain	chr19:22755564-24191440	19p12	chr19:22831403-22857036	1.18E-2	4.692	*ZNF723*
Gain	chr19:34477100-37895554	19q12-q13.11	chr19:34839864-34892756	7.50E-14	10.887	*PLEKHF1*, *C19orf12*
Gain	chr2:94793151-118939207	2q11.1-q14.2	chr2:95017289-95050247	2.00E-2	4.561	/
Gain	chr20:14929825-17414153	20p12.1	chr20:15505853-15529115	2.46E-3	5.069	*MACROD2*
Gain	chr20:51602600-51797590	20q13.2	chr20:51722390-51726725	1.26E-8	7.356	/
Gain	chr21:28466487-46944323	21q21.3-q22.3	chr21:43661758-43718330	1.27E-1	3.991	*SIK1*, *SIK1B*, *LINC00319*, *LINC01669*, *LINC00313*
Gain	chr3:169808488-171669472	3q26.2	chr3:170858670-171032269	7.64E-14	8.985	***MECOM***, *ACTRT3*, *MYNN*, *LRRC34*, *LRRIQ4*, *TERC*
Gain	chr4:61820279-64360471	4q13.1	chr4:64148793-64360471	4.12E-2	4.362	/
Gain	chr6:11306574-11952750	6p24.1	chr6:11470627-11545036	7.64E-4	5.340	*NEDD9*
Gain	chr6:71020557-74065543	6q13	chr6:72383552-72520206	1.88E-1	3.803	/
Gain	chr7:37375580-57890326	7p14.2-p11.1	chr7:53114918-53194448	3.47E-2	4.410	/
Gain	chr8:129370592-132726767	8q24.21-q24.22	chr8:129601251-129636803	7.64E-3	4.792	*LINC00824*
Gain	chr8:40154687-43910848	8p11.21-p11.1	chr8:40608933-40638501	6.65E-4	5.365	*ZMAT4*
Gain	chrX:61845481-67200492	Xq11.1-q12	chrX:61845481-62571001	2.22E-1	3.729	*SPIN4*, *LINC01278*
Loss	chr1:16797436-35789123	1p36.13-p34.3	chr1:27616247-27756094	8.88E-2	4.704	*WASF2*, *AHDC1*

SCNA Type	Genomic Coordinates (hg18) of Extended GISTIC Region	Location of Extended GISTIC Region	Genomic Coordinates (hg18) of Peak GISTIC Region	Q-bound for Peak Region	G-Score for Peak Region	Genes in Peak GISTIC Region
Loss	chr10:89251828-90869249	10q23.2-q23.31	chr10:89620956-89745318	1.03E-1	2.504	***PTEN***
Loss	chr16:33744011-34459363	16p11.2-p11.1	chr16:33744011-34319481	8.88E-2	2.860	*MIR9901, LOC112268173*
Loss	chr16:45205840-66994888	16q11.2-q22.1	chr16:58316118-58346135	8.88E-2	3.042	/
Loss	chr17:18083937-18771584	17p11.2	chr17:18558072-18591780	8.88E-2	3.474	*TRIM16L, FBXW10*
Loss	chr19:5166212-8072557	19p13.3-p13.2	chr19:7120029-7174340	1.46E-1	2.318	*INSR*
Loss	chr19:0-1654336	19p13.3	chr19:839331-876857	8.88E-2	4.636	*MED16, R3HDM4, KISS1R, RNU6-2*
Loss	chr2:141290607-142091845	2q22.1	chr2:141512334-141549533	2.41E-1	2.074	***LRP1B***
Loss	chr21:16104648-46944323	21q21.1-q22.3	chr21:25436494-25569678	2.04E-1	2.160	/
Loss	chr22:45341436-49106708	22q13.31-q13.33	chr22:48742080-48975222	8.88E-2	3.386	*PIM3, IL17REL, TTLL8, MLC1, MOV10L1, PANX2, TRABD, MIR6821**
Loss	chr4:115451731-141479193	4q13.31-q13.33	chr4:129663522-129691216	1.01E-1	2.528	/
Loss	chr4:181771427-182518809	4q34.3	chr4:182415084-182433256	8.88E-2	4.764	*LINC02500*
Loss	chr4:35651979-40878942	4p14	chr4:35780455-35831233	8.88E-2	3.203	*ARAP2*
Loss	chr5:59205723-59759773	5q12.1	chr5:59288399-59292832	8.88E-2	4.161	*PDE4D*
Loss	chr7:109360477-116122766	7q31.1-q31.2	chr7:109663496-109845497	8.88E-2	2.990	/
Loss	chr8:24314997-29040226	8p21.2-p21.1	chr8:26258130-26349606	1.19E-1	2.419	*PPP2R2A, BNIP3L*
Loss	chr9:25609706-28594341	9p21.2-p21.1	chr9:25926637-26889573	8.88E-2	3.058	*LOC100506422, CAAP1*
Loss	chr9:74060683-90190867	9q21.13-q22.1	chr9:78714346-78849837	8.88E-2	3.134	*FOXB2*
Loss	chrX:121101286-121546546	Xq25	chrX:121162142-121262032	8.88E-2	4.675	/

Consensus cancer genes (* Tier-1 COSMIC v90) are shown in bold

Table 5.

Extended and peak GISTIC regions identified among the "unspecified" molecular subgroup of EC

SCNA Type	Genomic Coordinates (hg18) of Extended GISTIC Region	Location of Extended GISTIC Region	Genomic Coordinates (hg18) of Peak GISTIC Region	Q-bound for Peak Region	G-Score for Peak Region	Genes in Peak GISTIC Region
Gain	chr1:176889044-247249719	1q25.2-q44	chr1:226520130-226684198	1.201E-2	1.625	*OBSCN, TRIM11, TRIM17, HIST3H3, MIR6742*
Gain	chr11:0-2278975	11p15.5	chr11:2262382-2277501	1.302E-2	1.174	*C11orf21*
Gain	chr16:25589827-32045466	16p12.1-p11.2	chr16:30005992-30178440	2.767E-2	1.076	*TBX6, YPEL3, GDPD3, MAPK3, CORO1A, BOLA2B, BOLA2, SLX1A, SLX1B, SULT1A3, SULT1A4, NPIPB13, NPIPB12, SLX1B-SULTA4, SLX1BA-SULT1A3*
Gain	chr17:46022175-71330793	17q21.33-q25.1	chr17:49051857-49099570	2.574E-2	1.083	/
Gain	chr19:32615675-37581903	19q12-q13.11	chr19:33868381-33998333	1.265E-2	1.180	/
Loss	chr16:34584567-35106851	16p11.1	chr16:34911034-35106851	1.563E-1	1.356	/
Loss	chr5:70715382-98608326	5q13.2-21.1	chr5:98552049-98608326	1.563E-1	1.100	/
Loss	chrX:13889477-58363397	Xp22.2-p11.1	chrX:29494339-29543664	1.563E-1	1.092	*IL1RAPL1, MIR4666B*